Original paper

Suppressing Dicer inhibits proliferation and contributes to cellular senescence, partially *via* a p21-associated senescence pathway

Chao-Wen Cheng[1,2], Wen-Fang Fang[3], Yea-Mey Yang[1], Jiunn-Diann Lin[4,5]

[1]Graduate Institute of Clinical Medicine, College of Medicine, Taipei Medical University, Taipei, Taiwan
[2]Traditional Herbal Medicine Research Center, Taipei Medical University Hospital, Taipei Medical University, Taipei, Taiwan
[3]Department of Family Medicine, Leader Clinic, Taipei, Taiwan
[4]Division of Endocrinology, Department of Internal Medicine, Shuang Ho Hospital, Taipei Medical University, New Taipei City, Taiwan
[5]Division of Endocrinology and Metabolism, Department of Internal Medicine, School of Medicine, College of Medicine, Taipei Medical University, Taipei, Taiwan

Dicer is known to engage in regulating micro (mi)RNA biosynthesis. However, the role in driving thyroid carcinogenesis is unknown.
In this study, we explored the role of Dicer in the carcinogenesis of well-differentiated thyroid carcinoma (WDTC). Thyroid cancer complementary (c)DNA and tissue arrays were purchased to measure Dicer messenger (m)RNA and protein levels. Additionally, research into silencing *Dicer1* in papillary thyroid cancer (PTC) (TPC-1), follicular thyroid cancer (FTC), and normal thyroid (Nthy-ori 3-1) cell lines was also applied to evaluate its effects on tumour behaviors.
Dicer1 mRNA was upregulated in PTC, while the Dicer protein was overexpressed in PTC and FTC tissues. Suppressing Dicer led to inhibition of cell proliferation in all cell lines, and repression of cell-cycle progression signatures in TPC-1 cells. Furthermore, p21 expression consistently increased in response to compromising Dicer in all four cell lines. Finally, *Dicer1*-knockdown TPC-1 and Nthy-ori 3-1 cells demonstrated nuclear phospho-H2AX staining, reduced bromodeoxyuridine incorporation ability, and G_1 phase arrest of the cell cycle.
Collectively, Dicer expression is increased in WDTC clinical samples, and Dicer regulates the proliferative ability of normal and WDTC cells, at least in part, through p21-dependent modulation of a cell-senescence mechanism linked to genomic instability.

Key words: well-differentiated thyroid cancer, papillary thyroid cancer, follicular thyroid cancer, Dicer.

Introduction

Thyroid cancer is the most prevalent endocrine tumour [1]. With the increasing utilization of thyroid ultrasonography to detect thyroid nodules in clinical settings, increasing numbers of thyroid carcinomas are being detected. Primary thyroid cancers are composed of several types, including well-differentiated thyroid carcinoma (WDTC), poorly differentiated thyroid carcinoma, anaplastic thyroid carcinoma (ATC), and medullary thyroid carcinoma (MTC). Well-differentiated thyroid carcinoma, including papillary thyroid carcinoma (PTC) and follicular thyroid carcinoma (FTC), has an excellent prognosis with

a 5-year survival rate of approximately 85-94%, but with a high disease recurrence rate of about 30-39% [2–4]. Most PTC and FTC are frequently recognized to harbor genetic alterations involved in the mitogen-activated protein kinase (MAPK) and phosphatidylinositol 3-kinase (PI3K)-Akt signaling pathways. In the meantime, poorly differentiated thyroid cancer and ATC accumulate genetic variations and are associated with an advanced disease course and unfavorable outcomes [1, 4]. On the other hand, MTC, derived from calcitonin-secreting C cells, accounts for about 4% of primary thyroid cancers. Medullary thyroid carcinoma is sometimes also associated with the germline rearranged during transfection proto-oncogene and multiple endocrine neoplasia type 2, and should be assessed for the possible presence of pheochromocytoma, hyperparathyroidism, Marfan syndrome, *etc*. [1, 4].

Micro (mi)RNA, a type of non-coding RNA with a short length, influences protein translation and regulates cell biological processes through binding to corresponding messenger (m)RNAs [5]. The RNase III endonuclease, Dicer, is engaged in the critical step of synthesizing mature miRNA, and is involved in multiple biological functions, including cell division, migration, differentiation, immunity, *etc*., and abnormal Dicer expression could contribute to multiple human disorders [5]. Accumulating evidence has shown that dysregulated *Dicer1* gene expression participates in the initiation and progression of various cancer types, and even affects treatment responses [6–9]. Recent reports showed that *Dicer1* germline mutations can lead to *Dicer1* syndrome, which contributes to susceptible individuals developing benign and malignant thyroid tumours from infancy [10]. At the same time, *Dicer1* germline and somatic mutations may also be associated with the occurrence of benign thyroid lesions and thyroid cancer [11–15]. Although the underlying mechanisms remain unclear, these clinical findings suggest that dysregulation of Dicer-dependent signaling pathways may contribute to aggressive features of thyroid pathology. Nevertheless, the precise role of *Dicer1* in initiating or modulating thyroid cancer evolution remains controversial. By utilizing cell experiments, Ramirez-Moya *et al*. [16] described how Dicer may exert a tumour-suppressive function in the pathogenesis of thyroid cancer, and downregulation of *Dicer1* gene expression could promote thyroid cancer aggressiveness. On the contrary, another *in vitro* study showed the oncogenic potential of thyroid cancer and described how *Dicer1* gene silencing could repress cell proliferation [17].

Given these conflicting findings, the mechanistic role of Dicer in the pathogenesis of WDTC still remains unclear. Therefore, this study aimed to examine the expression of Dicer in clinical thyroid tumours and to explore its functional significance in thyroid cancer cell proliferation and senescence. We evaluated differential expressions of Dicer mRNA and protein levels between WDTC and normal tissues, and associations of Dicer with clinical parameters were determined. Moreover, gene-silencing experiments were used in WDTC and normal thyroid cell lines to elucidate the possible role of Dicer in modulating malignant behaviors.

Material and methods

Thyroid cancer specimens

A TissueScan complementary (c)DNA microarray including 5 normal thyroid, 4 FTC, 4 Hürthle cell carcinoma (HCC), 1 ATC, 1 Hürthle cell adenoma, 1 MTC, and 32 PTC tissues at various clinical stages was purchased from OriGene Technologies (HTRT101, Rockville, MD, USA). In addition, a thyroid cancer tissue array was acquired from Super Biochip (CT1-L26, SuperBioChips Laboratories, Seoul, Korea), which included 9 normal thyroid, 8 FTC, 1 ATC, and 41 PTC samples at different stages and with different pathological features. However, as 3 normal and 4 PTC tissues were lost, therefore, only 6 normal thyroid and 37 PTC tissues were analyzed. The staging of thyroid cancer in the cDNA and tissue arrays was based on the cancer staging system published by the 7th American Joint Committee on Cancer [18]. This study did not involve either human participants or animal experiments.

Cell culture and transfection

Papillary thyroid cancer (TPC-1) and FTC (FTC-133 and FTC-236) cell lines, as well as a normal thyroid cell line (Nthy-ori 3-1; Nthy), were used in this study. Cell line authentication was performed on 26 November 2025 using short tandem repeat (STR) profiling (GenePrint 24 System, Tri-I Biotech, Inc., New Taipei City, Taiwan), confirming that all cell lines showed a 100% match to their reference STR profiles. In addition, all cell lines were routinely tested for mycoplasma contamination using a polymerase chain reaction (PCR) based mycoplasma detection kit, with the most recent test performed on 21 November 2025. Scrambled and two *Dicer1* short-hairpin (sh)RNA constructs were obtained from the National RNAi Core Facility (Institute of Molecular Biology/Genomic Research Center, Academia Sinica, Taipei, Taiwan). After puromycin selection (Invitrogen, San Diego, CA, USA), all cells were routinely cultured in Dulbecco's modified Eagle medium (DMEM; Invitrogen, Carlsbad, CA, USA) supplemented with 10% fetal bovine serum (FBS) in a humidified incubator containing 5% CO_2 at 37°C. The sequence of the *Dicer1*-KD1-shRNA oligonucleotide was 5'-CCGGGCTCGAAATCTTACGCAAATACTCGAG-

TATTTGCGTAAGATTTCGAGCTTTTTG-3', and that of the *Dicer1*-KD2-shRNA oligonucleotide was 5'-CCGGGCTGGCTGTAAAGTACGACTACTC-GAGTAGTCGTACTTTACAGCCAGCTTTTTG-3'.

Transcriptome profile analysis and transcript quantification

Cellular RNA was isolated using a GENEzolTM TtiRNA Pure Kit (Geneaid, New Taipei City, Taiwan), and first-strand cDNA (GoScript™ Reverse Transcription Mix, Oligo(dT), Promega, Madison, WI, USA) was prepared as previously described [19]. A quantitative PCR (qPCR) of target genes and housekeeping genes (b-actin [*actin*] or hypoxanthine-guanine phosphoribosyltransferase [*HPRT1*]) was performed using a mixture of 20 μl of buffer containing cDNA, SYBR green reagent (BIOTOOLS, Taipei, Taiwan), and each of the forward and reverse primers (6 μM). Mixtures were amplified in a real-time PCR instrument under the following conditions: initial step at 50°C for 2 min, followed by 95°C for 15 min and 45 cycles of melting at 95°C for 15 s, annealing at 55°C for 30 s, and extension at 72°C for 30 s. In each experiment, dissociation curves were performed to check the absence of nonspecific amplification and primer-dimer formation. The quantity of each product was measured using the formula $-\Delta Ct$, where $\Delta Ct = Ct$ (target) – Ct (*actin* or *HPRT1*). Supplementary Table SI displays the sequence of each paired primer.

To delineate the possible role of Dicer in inducing or promoting thyroid cancer, RNA samples were extracted from normal control (NC) and KD2 groups of the TPC-1 cell line. RNA library creation and sequencing were customized by Tools Biotech (BIOTOOLS). RNA-sequencing (RNA-Seq) data were collected using Expander 7 software [20]. Differential expressions of pre-established gene sets between the NC and KD2 groups were analyzed by the gene set enrichment assessment (GSEA) program. We first generated two ranked gene lists by obtaining multiples of change of these annotated genes in the KD2 group compared to the NC group, the GSEA program was subsequently utilized to determine possible activation or suppression of tumourigenic pathways in the KD2 group compared to the NC group. Hallmark gene sets available in the Molecular Signature Database (http://software.broadinstitute.org/gsea/msigdb) were used for further analysis. Analyzed gene sets with a normalized p (Norm p) value of < 0.05 and a false discovery rate of < 0.05 were considered to exhibit significant enrichment.

Immunostaining

Immunohistochemical staining of Dicer (anti-Dicer antibody, 1 : 200; ab259327, Abcam, Cambridge, UK) in thyroid tissues was performed using the Novolink Polymer Detection System (Leica Biosystems Newcastle Ltd., Newcastle, UK) as per the manufacturer's protocol. Immunofluorescence (IF) staining of phosphorylated histone H2A histone family member X (anti-phopho-H2AX antibody; AP0099, ABclonal Technology, New Taipei City, Taiwan) was performed in eight-well glass chamber slides. After seeding 1×10^3 cells/well for 48 h, cells were fixed with 4% buffered paraformaldehyde, endogenous peroxidase activity was blocked and quenched, and an anti-phospho-H2AX antibody with 1 : 200 dilution was added. Subsequently, an FITC-conjugated goat anti-rabbit IgG and 4',6-diami-dino-2 phenylindole (Vector Labs, Burlingame, CA, USA) was applied, and slides were observed by IF microscopy (Olympus CKX53 inverted microscope, Olympus Corporation, Tokyo, Japan).

Live/dead cell viability assay

Cells were seeded at 2×10^3 cells/well in 96-well plates, and the cell growth status was assessed with a live/dead cell viability assay every 24 h for up to 3 days. A MasterMix solution (50 ml containing 40 ml ethidium homodimer-1 [EthD1]), 8 ml Hoechst 33342 (20 mM), and 2 ml culture medium) was added to each well that contained 150 ml of medium to a final volume of 200 ml. Plates were incubated in the dark at room temperature for 30 min. Live cell counts ($Hoechst^+EthD\text{-}1^-$ cells), dead cell counts ($Hoechst^+EthD\text{-}1^+$ cells), and total cell counts ($Hoechst^+$ cells) were determined with the ImageXpress Pico Automated Cell Imaging System (Molecular Device, San Jose, CA, USA). Cell viability (%) in the live/dead cell viability assay was defined as (live cell counts/total cell counts) × 100%. Cell viability was also confirmed every 24 h by a colorimetric method of the CellTiter 96® AQueous One Solution Cell Proliferation Assay (3-(4,5-dimethylthiazol-2-yl)-5-(3-carboxymethoxyphenyl)-2-(4-sulfophenyl)-2H-tetrazolium – MTS) (Promega, Madison, WI, USA). After 48 h culture, 20 μl of MTS reagent was added to each well and incubated for 2 h at 37°C. The absorbance was measured at 490 nm using a microplate spectrophotometer (SpectraMax 190; Molecular Devices, Sunnyvale, CA, USA). Cell viability was calculated relative to the control group.

Colony-formation assay

Cells were seeded at 500 cells/well in six-well plates in cell medium with 10% FBS for 14 days at 37°C. Methanol (1 ml) was added to each dish for 3 min, crystal violet was added, and then the results were photographed. The colony size was determined as (total colony area/entire area) × 100% using ImageJ bundled with 64-bit Java 8 software (https://imagej.nih.gov/ij/download.html).

Wound-healing assay (cell-migration assay)

A wound-healing assay was performed by a documented method [21]. The wound-healing assay was performed by seeding 2×10^4 cells into each wound-produced culture insert (400 $\pm$50 μm, ibidi) and incubated overnight. The culture insert was removed after appropriate cell attachment and washed twice with phosphate-buffered saline (PBS), and 10% FBS medium was added. Cell migration toward the wounded area was observed (Olympus CKX53 inverted microscope, Olympus Corporation, Tokyo, Japan) and photographed at different times for 17 h.

Western blot analysis

Cells was first treated with lysis buffer, containing 50 mM Tris-HCl (pH 7.4), 0.1 mM EDTA, 0.1 mM ethylene glycol tetraacetic acid 12 mM β-mercaptoethanol, 1 mM phenylmethylsulfonyl fluoride (PMSF, Sigma, St. Louis, MO, USA), 1 ml/ml aprotinin, and 1 mg/ml leupeptin. After centrifugation at 12,000 $\times$ *g* for 15 min at 4°C, the supernatant was collected, and the protein concentration was determined using the Bradford method (BioRad, Hercules, CA, USA). Thirty micrograms of tissue protein was separated by sodium dodecylsulfate polyacrylamide gel electrophoresis, and then transferred to nitrocellulose membranes (Millipore, EMD Millipore Corp., Billerica, MA, USA). After blocking with blocking solution containing 5% skim milk and 1% bovine serum albumin in 0.1 M PBS, the membrane was probed with primary antibodies. The primary antibodies used are listed as the followings: anti-Dicer antibody (1 : 200; ab259327, Abcam, Cambridge, UK), anti-p21 antibody (1 : 500; A19094, ABclonal Technology, New Taipei City, Taiwan); anti-p16 antibody (1 : 1000, #68410, Danvers, Massachusetts, USA), anti-p53 antibody (1 : 500; A22449, ABclonal Technology, New Taipei City, Taiwan), and anti-GAPDH antibody (1 : 5000, GTX100118,GeneTex, Irvine, California, USA). The membrane was subsequently incubated with a goat anti-rabbit antibody (Dicer, p21, p53 and GAPDH) antibody (1 : 1000, 111-035-003, Jackson ImmunoResearch Laboratories, West Grove, USA), and anti-mouse antibody (p16, 1 : 5000. 115-055-003, Jackson ImmunoResearch Laboratories, West Grove, USA). The western blot results were quantified by using ImageJ bundled with 64-bit Java 8 software.

Flow cytometry

The cell cycle was evaluated based on a standard protocol reported by Cecchini *et al*. [22]. After being released from cell synchronization for indicated time points, cells were harvested and fixed with cold 70% alcohol at 4°C for 30 min. Then cells were re-suspended in staining buffer containing PBS with 100 mg/ml RNase A (Geneaid, RA500050; New Taipei City, Taiwan) and 50 mg/ml propidium iodide (PI, P4170; Sigma-Aldrich, Billerica, MA, USA) at 4°C overnight, and cells were analyzed with a Muse® Cell Analyzer (Merck, Darmstadt, Germany).

Bromodeoxyuridine assay

A bromodeoxyuridine (BrdU) assay was performed according to the manufacturer's protocol (Roche Diagnostics, Mannheim, Germany) [23]. Cells were seeded at 5×10^3 cells/well in 96-well plates and incubated at 37°C. After 40 h of starvation, 10 ml of a BrdU labeling solution in 10% FBS was added to each well, and incubated at 37°C for 24 h. Later, 200 ml of a denaturing solution was added to each well and incubated at room temperature for 30 min. After removing the solution, 100 ml of a detection antibody solution was added to each well, incubated at room temperature for 90 min. Cells were next treated with a substrate solution containing tetramethylbenzidine at 100 ml/well for incubation at room temperature for 5 min, and 25 ml of a stop solution with 1 N HCl was added to each well. Finally, the absorbance at 450 nm was determined with a spectrophotometer (SpectraMax 190; Molecular Devices, Sunnyvale, CA, USA).

Statistical analysis

All statistical analyses were conducted using SPSS software, ver. 18.0 (IBM, Armonk, NY, USA). Quantitative values are shown as the mean $\pm$ standard error or median (range). A χ^2 test or Fisher's exact test was used to analyze associations with categorical data. Student's *t*-test was used to assess differences in continuous data between two different groups. Differences among multiple groups were determined by a one-way analysis of variance (ANOVA) and using the Bonferroni *post hoc* test. All statistical tests were two-sided, and $p < 0.05$ was considered significant.

Results

Differential expressions of *Dicer1* mRNA and protein levels in normal thyroid and thyroid cancer tissues

In examining mRNA expression levels in a thyroid cancer cDNA array, *Dicer1* mRNA levels were significantly higher in PTC tissues than in NC tissues ($p = 0.027$) (Figure 1A). Meanwhile, there were no significant differences in *Dicer1* mRNA levels between the FTC and HCC groups (Figures 1B, C). In addition, *Dicer1* mRNA levels were associated with smaller changes in the tumour extent, lymph node (LN) metastasis, and staging in PTC (Figures 1D–F).

For Dicer protein measurements in a commercial tissue microarray, 52 tissues in total were analyzed, as four PTC and three normal thyroid tissues were

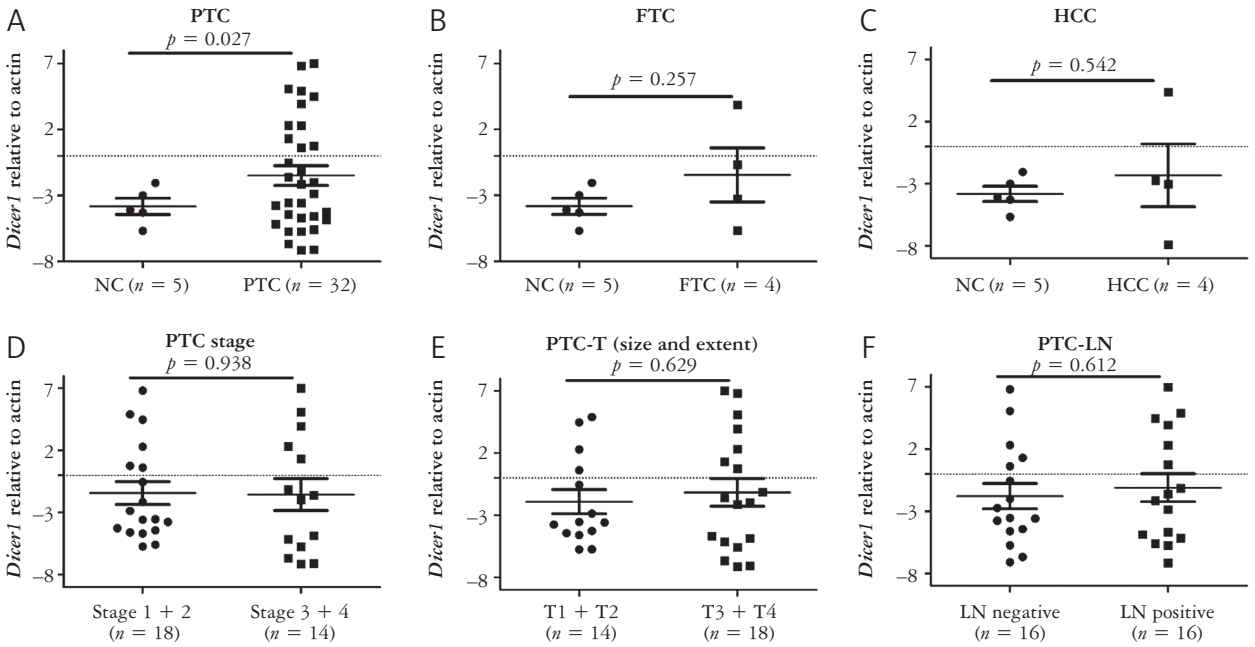

Figure 1. Differential *Dicer1* mRNA levels in normal and papillary thyroid carcinoma (**A**), follicular thyroid carcinoma (**B**), and Hürthle cell carcinoma (**C**), and associations of *Dicer1* mRNA expression with tumour size and extent (**D**), lymph node invasion (**E**) and tumour staging (**F**)

FTC – follicular thyroid cancer, HCC – Hürthle cell carcinoma, NC – normal control, PTC – papillary thyroid cancer
Each bar indicates the mean ± standard error. $p < 0.05$ indicates statistical significance.

missing. Figures 2A–D, respectively, demonstrate that PTC at stages I, II, III, and IV exhibited generally elevated Dicer protein levels in the cytoplasm compared to normal thyroid tissues, which are shown in Figures 2H, I, and Supplementary Figure S1A. At the same time, FTC at stages I and II, and ATC also expressed profound Dicer protein expression, as respectively demonstrated in Figures 2E–G and Supplementary Figure S1B. However, there were no significant correlations of Dicer protein expressions with PTC (Supplementary Figure S1C) or FTC staging.

Silencing *Dicer1* expression suppressed cell viability and growth in normal thyroid and thyroid cancer cell lines

To further assess the influence of Dicer levels in modifying malignant behaviors in WDTC, normal and WDTC cell lines, including the Nthy, TPC-1, FTC-133, and FTC-236 cell lines, were used for *in vitro* experiments. In addition, two divergent *Dicer1* shRNA clones, KD1 and KD2, were utilized to assess the effects on cell viability and growth. Both KD1- and KD2-shRNA expressing cell lines showed a marked decrease in *Dicer1* mRNA expression compared to the scrambled clone-expressing cells in all four cell lines (Supplementary Figures S2A–D). After *Dicer1* was knocked down by either KD1- or KD2-shRNA, even dead cell numbers increased; however < 1.5% of cell viability was altered (Figures 3A–D). Meanwhile, live cell numbers were significantly reduced in *Dicer1*-knockdown cells, implying a possible role of Dicer in regulating cell growth but not in promoting cell death (Figures 3A–D).

In the MTS and colony-formation assays, we further assessed the impact of repression of *Dicer1* on the cell-growth ability of Nthy and TPC-1 cells. Both KD1- and KD2-shRNA-expressing Nthy and TPC-1 cells displayed significant decreases in the cell-proliferation ability, with a more profound diminution in KD2- than in KD1-shRNA in the TPC-1 cell line (Figures 4A, B). Moreover, silencing of *Dicer1* in both Nthy and TPC-1 cells resulted in reduced colony-formation abilities, and KD2-shRNA also showed a greater reduction compared to KD1-shRNA in both the Nthy and TPC-1 cell lines (Figures 4C–E). Meanwhile, the cell-migratory ability did not significantly change after Dicer was suppressed in the TPC-1 and Nthy cell lines (Supplementary Figures S3A, B). These findings indicated that downregulation of Dicer led to significant suppression of cell growth but did not influence cell mobility in either normal or thyroid cancer cells.

Silencing of *Dicer1* led to upregulation of p21 mRNA and inhibition of cell cycle-related signatures

In order to further elucidate the possible mechanisms of Dicer in regulating thyroid carcinogenesis, NC and KD2-shRNA-expressing TPC1 cells were applied for a transcriptomic analysis by next-generation

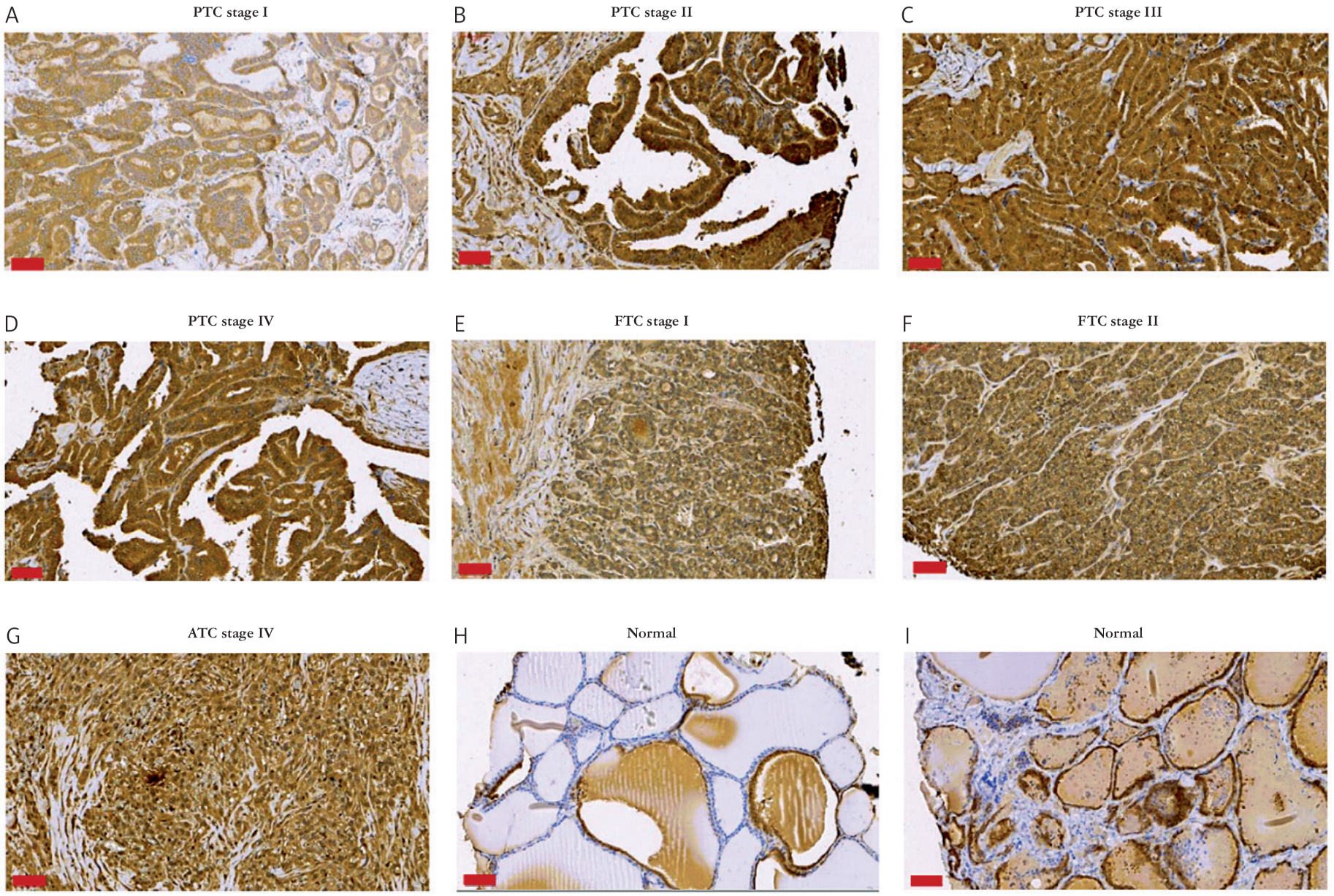

Figure 2. Dicer protein expressions in various thyroid tumours. Overexpression of the Dicer protein in papillary thyroid cancer at stages I (**A**), II (**B**), III (**C**), and IV (**D**) (100×). Upregulation of the Dicer protein in follicular thyroid cancer at stages I (**E**) and II (**F**) (100×). **G**) Anaplastic thyroid cancer also demonstrated distinct Dicer protein staining. **H, I**) Two normal thyroid tissues with focal and abundant Dicer staining

ATC – anaplastic thyroid carcinoma, FTC – follicular thyroid cancer, PTC – papillary thyroid cancer
The red column is a scale bar = 100 μm.

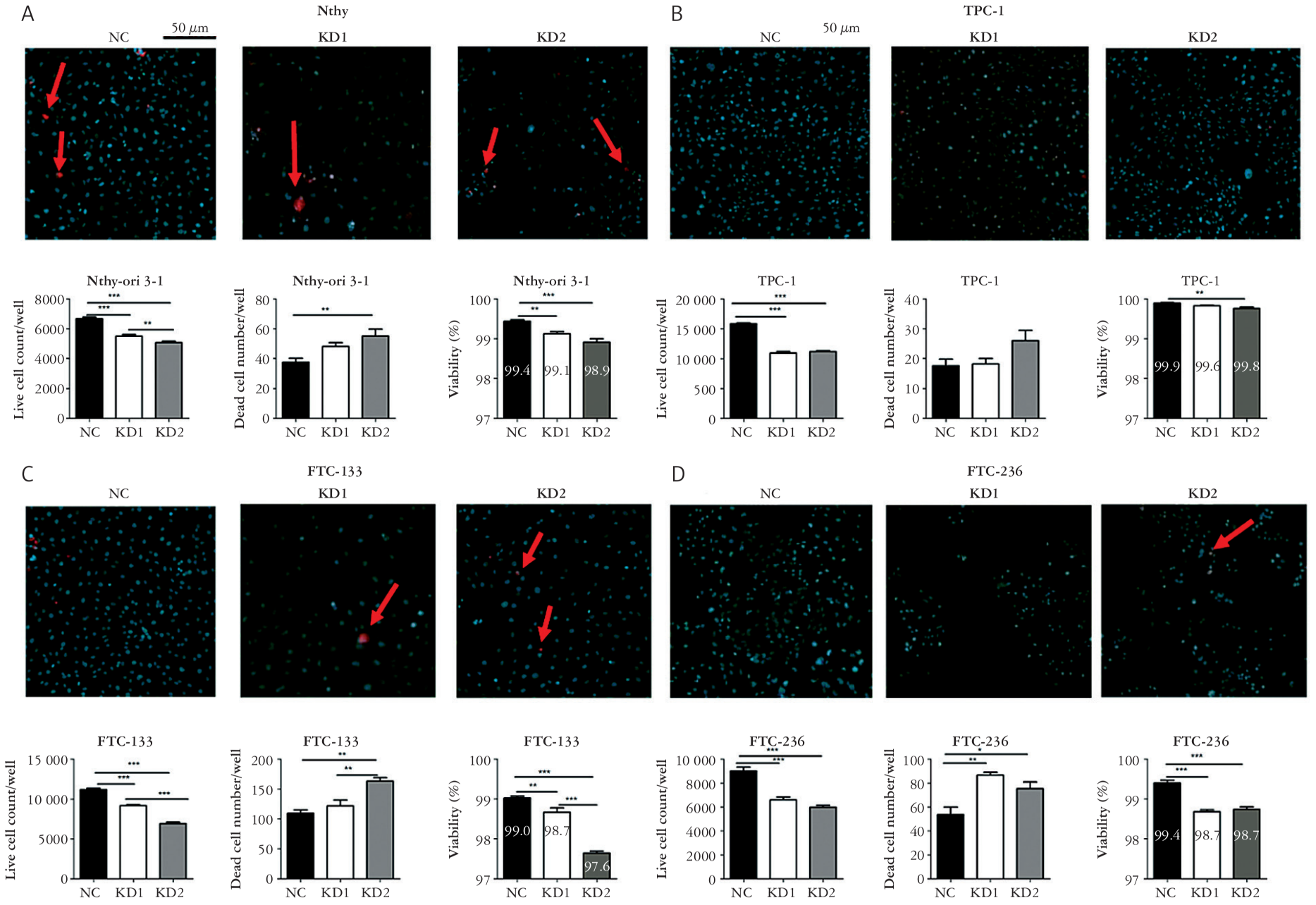

Figure 3. Live cell and dead cell counts, and cell viability after *Dicer1* silencing in the normal thyroid (Nthy-ori) 3-1, TPC-1, FTC-133, and FTC-236 cell lines. Comparisons of viable cell images and viability among the normal control, and KD1-shRNA- and KD2-shRNA-expressing Nthy-ori 3-1 (Nthy) (**A**), TPC-1 (**B**), FTC-133 (**C**), and FTC-236 cells (**D**)

FTC – follicular thyroid cancer, NC – normal control, Nthy-ori – normal thyroid.
*Cell viability (%) was defined as (live cell counts/total cell counts) × 100%. Blue (Hoechst+EthD-1-) indicates live cells and red (Hoechst+EthD-1+) indicates dead cells. Each bar indicates the mean ± standard error. * $p < 0.05$; ** $p < 0.01$; *** $p < 0.001$.*
The red column is a scale bar = 50 μm.

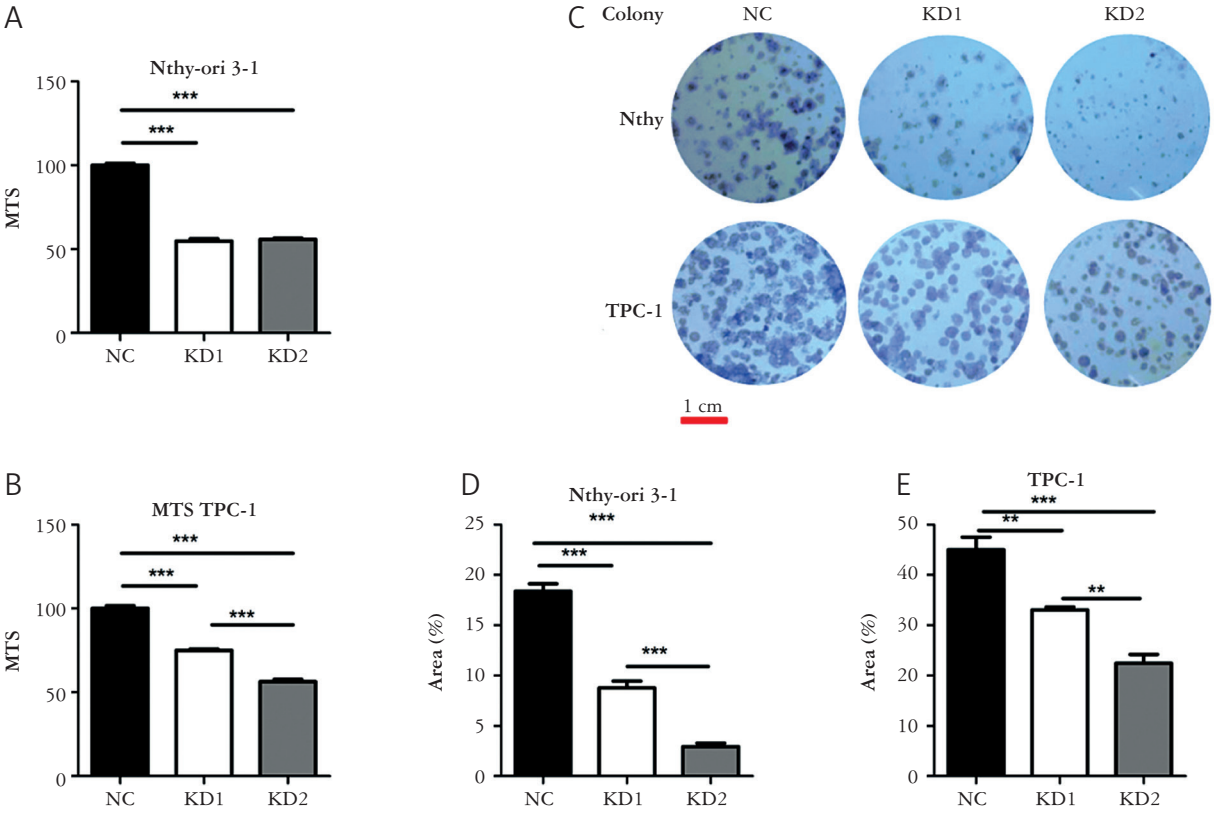

Figure 4. Cell proliferation after compromising Dicer in the normal thyroid (Nthy-ori) 3-1 and TPC-1 cell lines. MTS results among the three clones in Nthy (**A**) and TPC-1 cells (**B**). Colony-formation results after *Dicer1* (**C**) was silenced in the Nthy (**D**) and TPC-1 cell lines (**E**)

MTS – 3-(4,5-dimethylthiazol-2-yl)-5-(3-carboxymethoxyphenyl)-2-(4-sulfophenyl)-2H-tetrazolium, NC – normal control, Nthy-ori – normal thyroid
*Each bar indicates the mean ± standard error. *p < 0.05; **p < 0.01; ***p < 0.001.*
The red column is a scale bar = 1 cm.

Table I. Results of a gene set enrichment assessment of *Dicer1* knockdown in the TPC-1 cell line

Altered signatures	ES	NES	Nom *p*-value	FDR *q*-value
Downregulated pathways				
HALLMARK_G_2M_CHECKPOINT	–0.549	–2.427	< 0.001	< 0.001
HALLMARK_E2F_TARGETS	–0.521	–2.3430	< 0.001	< 0.001
HALLMARK_MYC_TARGETS_V2	–0.547	–1.982	< 0.001	0.001
HALLMARK_MITOTIC_SPINDLE	–0.364	–1.659	< 0.001	0.013
Upregulated pathways				
HALLMARK_INTERFERON_ALPHA_RESPONSE	0.513	1.822	0.001	0.012
HALLMARK_P53_PATHWAY	0.427	1.665	< 0.001	0.044

ES – enrichment score, FDR – false discovery rate, NES – normalized enrichment score, Nom – normalized
Nom p value of < 0.05 and FDR of < 0.05 were considered significant.

sequencing (RNA-Seq). In the GSEA analysis, after *Dicer1* was knocked down by KD2-shRNA, several signaling pathways were inhibited, including the G_2M checkpoint, E2F target, Myc-target V2, and mitotic spindles, and results are shown in Table I and Figure 5A. In the meantime, suppression of Dicer provoked interferon a and p53 signaling pathways (Table I). In the meantime, multiple well-known tumourigenic signatures, including KRAS, PI3K-Akt-mammalian target of rapamycin (mTOR), epithelial-to-mesenchymal transition (EMT), angiogenesis, Notch, and Wnt-b-catenin, were not altered (data not shown).

Furthermore, RNA-Seq level alterations of individual genes in four depressed hallmark signatures after silencing of *Dicer1* were analyzed. In the transcriptomic profile analysis, *p21* and Ki-67 RNA-Seq levels displayed the most significant changes among

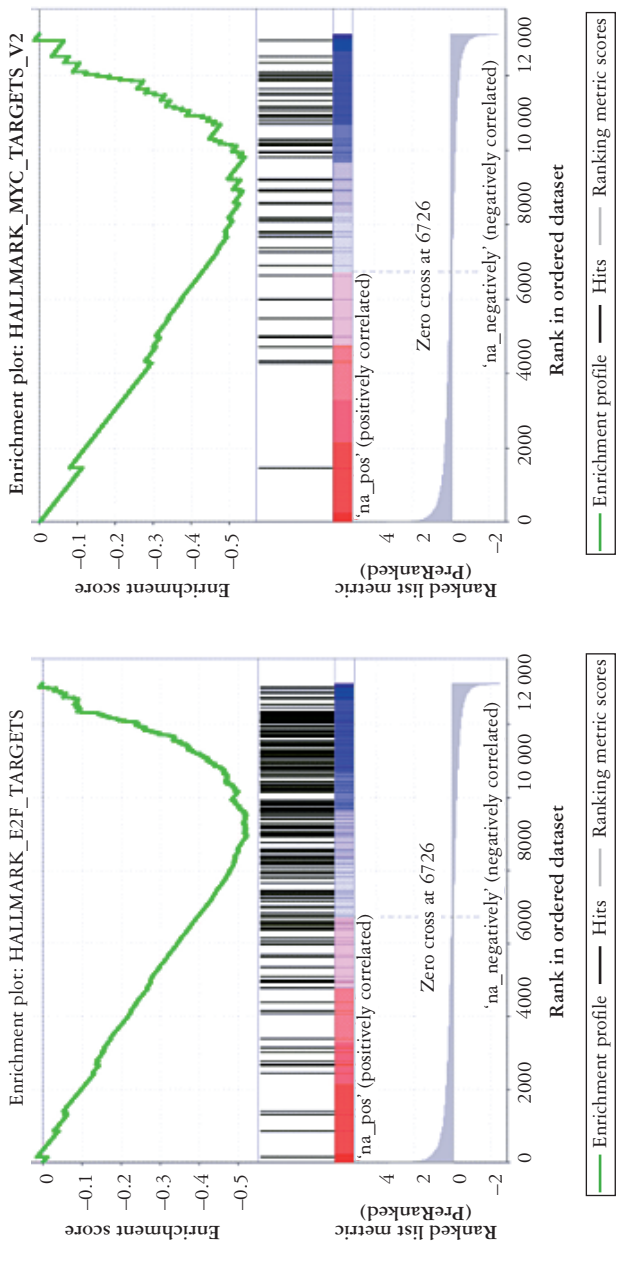

Figure 5. Enrichment plot of a gene set enrichment assessment (GSEA) of *Dicer1*-knockdown in the TPC-1 cell line and alterations of *Dicer1*, p21, and Ki-67 mRNA levels in the normal thyroid (Nthy-ori) 3-1 and TPC-1 cell lines after *Dicer1* was silenced. **A)** The enrichment plots of the GSEA for top three suppressed signaling pathways, including HALLMARK_G2_M_CHECKPOINT, HALLMARK_E2F_TARGETS, and HALLMARK_MYC_TARGET_V2. The enrichment score (ES) derived from the correlation between the gene set and the queried gene signatures was plotted as the green curve. **B)** *Dicer1*, p21, and Ki-67 mRNA levels in Nthy-ori 3-1 cells. **C)** Expressions of *Dicer1*, p21, and Ki-67 mRNA levels in TPC-1 cells

NC – normal control, Nthy-ori – normal thyroid
*Each bar indicates the mean ± standard error. *p < 0.05, **p < 0.01, ***p < 0.001.*

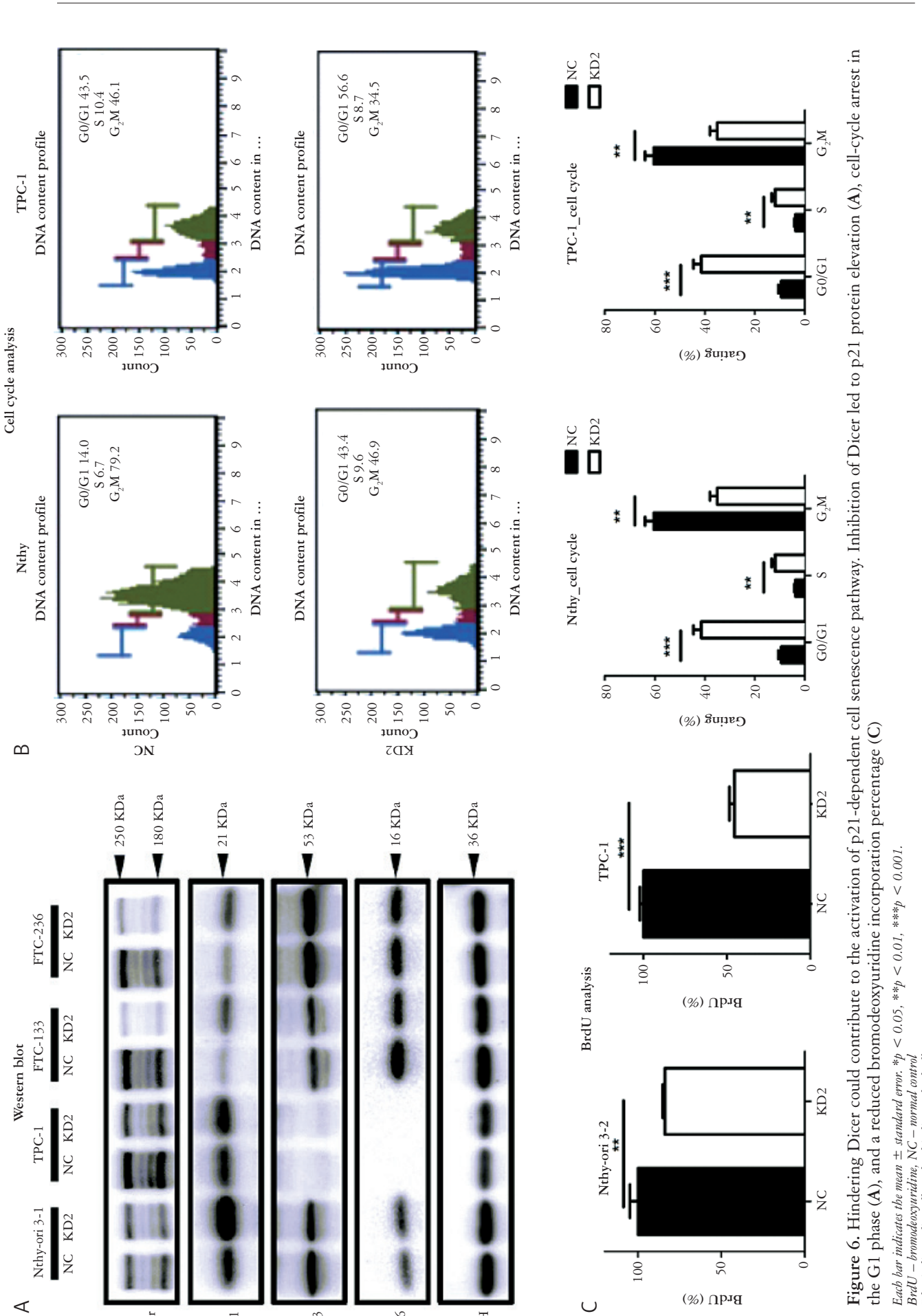

Figure 6. Hindering Dicer could contribute to the activation of p21-dependent cell senescence pathway. Inhibition of Dicer led to p21 protein elevation (**A**), cell-cycle arrest in the G1 phase (**A**), and a reduced bromodeoxyuridine incorporation percentage (**C**)

*Each bar indicates the mean ± standard error. *$p < 0.05$, **$p < 0.01$, ***$p < 0.001$.*
BrdU – bromodeoxyuridine, NC – normal control
Blue indicates live cells and red indicates dead cells.

all of the analyzed markers between these two groups. *Dicer1, p21,* and Ki-67 mRNA expression levels were further measured using a qPCR method in different cell lines, and *p21* mRNA increased in KD2-shRNA-expressing cell lines (Figures 5B, C, Supplementary Figures S4A, C). Meanwhile, Ki-67 mRNA significantly decreased in KD2 shRNA-expressing Nthy, FTC-133 and FTC-236 cells (Figures 5B, C, Supplementary Figures S4B, D). Although no significant differences in Ki-67 mRNA levels were observed between TPC-1 cells (Figure 5C), KD2-shRNA-expressing cells showed a slight decrease.

Blocking Dicer contributed to DNA damage, p21 protein upregulation, DNA synthesis inhibition, and cell-cycle arrest

It is known that p21 activation can lead to cell senescence and further result in cell-cycle arrest, inhibition of cell division, and limits normal cell and tumour growth [24]. To further elucidate the role of *Dicer1* in regulating cell senescence, several key markers, including the p21, p16, and p53 proteins, were quantified. In the basal condition, TPC-1, FTC-133, and FTC-236 cells showed greater Dicer protein expressions than Nthy cells (Figure 6A). Meanwhile, the p21 protein was more abundant in Nthy and TPC-1 cells than in FTC-133 and FTC-236 cells (Figure 6A), but the p16 and p53 proteins were undetectable in the TPC cell line (Figure 6A). After silencing *Dicer1*, consistent with the results of *p21* mRNA expression, the p21 protein was consistently higher in all cells (Figure 6A). Meanwhile, there were no obvious differences in p16 or p53 protein levels between NC and KD2-shRNA-expressing cells in the four cell lines (Figure 6A). In addition, compared to NC cells, repression of *Dicer1* restrained Nthy and TPC-1 cells to the G_1 phase in the cell-cycle analysis (Figure 6B). Moreover, percentages of BrdU incorporation also significantly decreased in *Dicer1*-silenced Nthy and TPC-1 cells, which suggested that DNA synthesis and entry into the S phase were also diminished after *Dicer1* was knocked down (Figure 6C). In addition, an IF method was utilized to detect phosphorylation of the histone H2AX protein, a classic marker of DNA damage. Compared to NC cells, KD2-shRNA-expressing Nthy and TPC-1 cells demonstrated strong nuclear phospho-H2AX staining, implying that Dicer suppression led to DNA damage (Supplementary Figure S5).

Discussion

Dicer plays a crucial role in processing miRNA and subsequently regulates translational processes and further modulates cell behaviors and phenotypes. Dysregulated *Dicer1* expression has been extensively investigated in multiple types of malignancies and is linked to tumour initiation and propagation, including lung, colon, oral, liver, breast cancers, *etc*. [6–9, 25]. *Dicer1* germline mutation (*Dicer1* syndrome) could be associated with the occurrence of 30 distinct neoplasms [26]. Reyes-Castro *et al*. [27] have reported that phosphorylated nuclear-Dicer could facilitate lung tumour progression in a mouse model. In addition, recent publications have shown that Dicer could exhibit a potential role in the R loop nucleic acid structure formation, and subsequently contributes to the tumourigenesis [28]. However, the effects of imbalanced *Dicer1* expression in thyroid carcinogenesis are conflicting. Erler *et al*. [29] examined 22 normal thyroid and 49 PTC samples, and described that *Dicer1* mRNA levels were diminished while Dicer protein expressions divergently increased in PTC samples. In addition, they also showed that lower *Dicer1* mRNA expressions were correlated with clinically advanced features. In contrast, by analyzing thyroid tissues, including 6 normal thyroid and 31 PTC samples, Penha *et al*. [17] reported that *Dicer1* transcripts were upregulated, but the protein was paradoxically reduced in PTC tissues. After analyzing 49 FTC and 10 normal thyroid tissues, Paulsson *et al*. [30] disclosed that both *Dicer1* mRNA and Dicer protein levels were reduced in FTC. In the present study, we demonstrated that both *Dicer1* transcripts and protein were upregulated in PTC; however, we showed no significant associations of *Dicer1* mRNA or protein levels with clinical parameters.

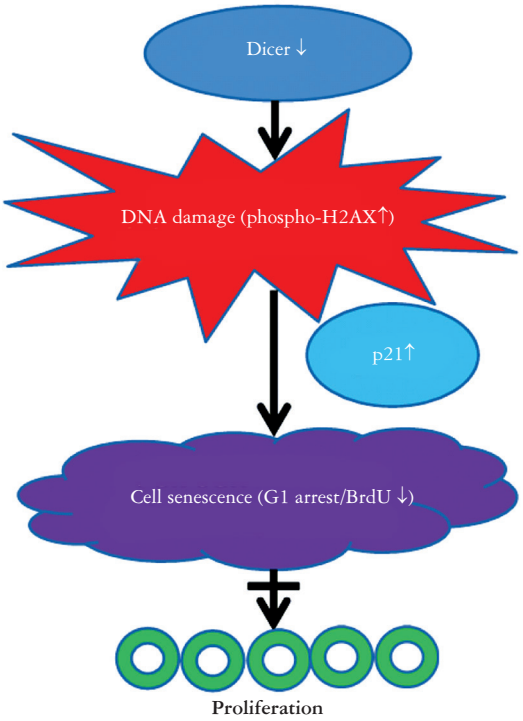

Figure 7. The postulated mechanism of suppressing Dicer inhibits cell proliferation, partially *via* p21 dependent pathway

BrdU – bromodeoxyuridine

The effects of Dicer in facilitating thyroid cell division also remain under debate. Two studies demonstrated that diminished Dicer expression promoted cell proliferation in normal and thyroid cancer lines, and suggested that *Dicer1* could act as a tumour-suppressor gene in thyroid tumourigenesis [16, 30]. By contrast, Frezzetti *et al*. [31] showed that *Dicer1*-knockout mice had smaller-sized thyroid glands compared to the control group, which indicated that Dicer was implicated in thyroid cell growth. In addition, Penha *et al*. [17] disclosed that Dicer exerted tumourigenic activity and provoked thyroid cell growth in a rat thyroid and TPC-1 cell line using both loss- and gain-of- function techniques. Our data showed that after Dicer was suppressed, cell viability was consistently blocked in the Nthy, TPC-1, FTC-133, and FTC-236 cell lines, and the cell-proliferative capacity was reduced in the Nthy and TPC-1 cell lines. Our *in vitro* study results were contradictory to those by Ramirez-Moya *et al*. [16] and Paulsson *et al*. [30] which showed Dicer displays a tumour-suppressive ability but in line with those reported in most cancer types and those reported in a publication by Penha *et al*. [17]. However, the cell-expansion analyses, including MTS and colony-formation assays, were conducted only in TPC-1 and Nthy cells; including FTC-133 and FTC-236 in cell-proliferation assays would further strengthen the conclusions. Moreover, the actual mechanism of the discrepant results between the present and other studies is unclear, and could possibly be attributed to intracellular Dicer levels, cell subtypes, tumour microenvironments, and experimental methods [5, 32]. Swahari *et al*. [32] reported that partial suppression of Dicer induces oncogenesis, while complete *Dicer1*-knockout leads to extensive DNA damage with resultant tumour suppression. In addition, Penha *et al*. [17] also hypothesized that Dicer can control thyrocyte proliferation only under favorable intracellular Dicer levels, and divergent Dicer intracellular levels after Dicer manipulation in different studies could have contributed to the discrepancy. On the other hand, evidence shows that a hypoxic environment can modulate Dicer in regulating diverse tumour progression or inhibition, suggesting the modulation of the tumour microenvironment by Dicer in regulating tumour behavior [33–35].

On the other hand, no significant associations of *Dicer1* mRNA and protein levels with clinical manifestations in PTC, including tumour staging and LN metastasis, were detected in this study. In addition, the cell-migratory ability did not significantly change after Dicer was suppressed in the TPC-1 and Nthy cell lines (Supplementary Figure S3). These data suggest that the fundamental role of Dicer could be in promoting normal and thyroid cancer cell growth. Dysregulated Dicer expression could lead to an increased tumour load, while it may play a less-important role in tumour invasiveness and metastasis in WDTC development, which were compatible with results in the clinical specimen study. Upregulated Dicer in PTC and FTC tissues irrespective of clinical parameters may imply that Dicer dysregulation could mainly be associated with tumour initiation and cell proliferation during thyroid carcinogenesis, rather than tumour invasion and metastasis, which are mainly present in later stages. Therefore, the findings from specimens and cell experiments might also imply the therapeutic potential of Dicer suppression in managing WDTC. Optimally blocking Dicer expression in WDTC at the early stage rather than at the late stage by developing a Dicer inhibitor could suppress tumour growth in clinical settings.

In the transcriptomic next-generation sequencing analysis, we observed that the top two indicators changed most profoundly among all biomarkers after Dicer-suppressed TPC1 cells exhibited p21 upregulation and Ki-67 downregulation. Interestingly, both p21 and Ki-67 are known to be linked to regulation of the cell cycle, cell senescence, and cell replication, and elevated p21 together with diminished Ki-67 highly implies that inhibiting Dicer contributed to cell-cycle interruption, cell-growth arrest, and possibly to cell senescence. In addition, in the GSEA, *Dicer1*-silenced TPC-1 cells only exhibited cell cycle-related pathways, with suppression of G_2M-, E2F-, and Myc-target-V2, and mitotic spindles, while the well-documented tumourigenic pathways, including Kras (MAPK), PI3K-Akt-mTOR, tumour invasion and migration (EMT), *etc*., were not altered. These GSEA findings further supported findings of the cell biological behavior in cell experiments, and indicated that dysregulated Dicer expression could stimulate thyroid tumourigenesis chiefly through modulating cell duplication and the cell cycle rather than regulating other carcinogenic signaling pathways. On the other hand, *Dicer1*-silenced Nthy and TPC-1 cells showed reduced Ki-67 mRNA levels, but this only reached statistical significance in the Nthy cell line. Aberrant activation of multiple biological pathways may contribute to this phenomenon, which could enhance Ki-67 expression and tumour growth in cancer cells. Therefore, we speculated that the influence of Dicer in regulating Ki-67 expression in PTC could be less prominent than in normal thyrocytes [36, 37].

Under physiological conditions, normal somatic cells always stop dividing and are restrained in the G_1 phase of the cell cycle after reaching a certain level of cell division, which is defined as cellular senescence. This physiological stasis is regarded as an important defensive mechanism to limit permanent cell and tumour growth. However, in the process of tumour development, certain cancer cells can evade this proliferation-impeding mechanism and subsequently re-enter the cell cycle, which ultimately leads to further cancer growth [38]. Evidence has shown that in addition to the aging process, multiple extrinsic

and pathological triggering factors, including oxidative stress, oncogenic stimulation, *etc*., can contribute to DNA damage, followed by excitation of the cell-senescence pathway [24]. The cell-senescence process is mainly mediated through either a p21- or p16-dependent pathway. p21, one member of the cyclin-dependent kinase (CDK) inhibitor family, can block the cell cycle through the G_1/S phase *via* binding with CDK2 [38]. The RNA-sequencing and GSEA analyses showed that inhibiting Dicer expression led to upregulation of p21 and cell cycle-associated signatures, which suggested that dysregulated Dicer is engaged in regulating thyroid carcinogenesis possibly *via* a p21-dependent cell-senescence mechanism. In the present study, after silencing *Dicer1*, in addition to elevated p21, the DNA damage marker, phospho-H2AX, also increased in TPC-1 and Nthy cells. Moreover, compromising Dicer expression in Nthy and TPC-1 cells was associated with G_1 phase arrest of the cell cycle and a reduction in the percentage of cells entering the S phase. Taken together, we assumed that *Dicer1*-knockdown leads to DNA damage, subsequently resulting in increased p21 protein levels, thus contributing to cell-cycle arrest at the G_1 phase and hindering cell-cycle progression to the S phase, ultimately promoting cell senescence and limiting cell and tumour growth. In addition to the absence in TPC1 cells, p16 and p53 proteins also showed smaller alterations after Dicer was inhibited in all other cell lines. These findings supported Dicer possibly participating in controlling the entry of DNA damage-mediated cell senescence and maintaining cell proliferation, potentially *via* p21-dependent, but p16- and p53-independent, mechanisms. However, to support a causal relationship between Dicer suppression and p21-dependent mechanism, further experiments are necessary, such as the combined silencing of *Dice1* and *p21*, or immunoprecipitation assays to investigate functional or physical interactions.

In the present study, we demonstrated that Dicer was upregulated in PTC and FTC clinical samples, and our findings also provide new insight into the functional consequences of Dicer dysregulation in thyroid cancer. The postulated mechanism is shown in Figure 7. Dysregulated Dicer impairs thyroid cancer cell stability, induces a DNA damage response evidenced by increased phospho-H2AX and p21 levels, which subsequently induces G1 phase arrest and reduces DNA synthesis, phenotypes consistent with a senescence response across both normal and malignant thyroid cell lines. These results connect miRNA-processing machinery to cell-cycle regulation and genomic stability in WDTC. By integrating transcriptomic profiling with functional assays, this study highlights a previously underappreciated link between Dicer-mediated RNA processing and p21-driven tumour cell senescence.

Study limitations

This study has several limitations. First, the analyses were performed mainly on commercial cDNA and tissue arrays with a relatively small sample size and the inherent heterogeneity within the thyroid cancer subgroups, which limited the ability to evaluate correlations with clinical outcomes such as tumour grade or disease stage. Larger cohorts with increased sample sizes and well-balanced subgroups are necessary to further elucidate its clinical relevance. Second, functional validation was restricted to *in vitro* models, and the absence of *in vivo* studies prevents definitive conclusions regarding the physiological relevance of Dicer suppression. Third, certain key phenotype-specific assays, including β-galactosidase staining, were not performed in this study. As these assays are essential to support senescence modulation, their absence may limit the reliability of our findings. Future studies quantifying additional senescence markers would make our conclusions more convincing. Fourth, mechanistic experiments such as double knockdown of *Dicer1* and *p21* or rescue assays were not performed; therefore, the proposed p21-related mechanism remains correlative. Future studies using patient-derived xenografts or genetically engineered mouse models, together with multi-omic profiling, will be essential to delineate whether Dicer exerts a context-dependent tumour-promoting or tumour-suppressive role in thyroid carcinogenesis.

Conclusions

Higher levels of the *Dicer1* protein were found in PTC and FTC clinical samples, but they were not related to any clinical parameters in PTC, and their central biological function was regulating thyroid cell proliferation. Silencing *Dicer1* repressed the proliferative ability of normal, PTC, and FTC cells partially by way of a p21-dependent cell-senescence mechanism linked to genomic instability. Although the long-term impact of *Dicer1* on thyroid cancer evolution cannot be directly inferred from our current data, these findings highlight its potential role in maintaining genomic integrity. Our study provides important insights into the biological function of *Dicer1* in thyroid cells and suggests that further investigation is warranted to explore its potential as a therapeutic target.

Disclosures

1. Institutional review board statement: This work was supported by a grant from the National Science and Technology Council, Taiwan (NSTC 112-2314-B-038-066).
2. Assistance with the article: The Graduate Institute of Clinical Medicine, College of Medicine, Taipei

Medical University, provided all instruments for this laboratory work.
3. Financial support and sponsorship: None.
4. Conflicts of interest: None.

References

1. Boucai L, Zafereo M, Cabanillas ME. Thyroid cancer: a review. JAMA 2024; 331: 425-435.
2. Seib CD, Sosa JA. Evolving understanding of the epidemiology of thyroid cancer. Endocrinol Metab Clin North Am 2019; 48: 23-35.
3. Prete A, Borges de Souza P, Censi S, Muzza M, Nucci N, Sponziello M. Update on fundamental mechanisms of thyroid cancer. Front Endocrinol (Lausanne) 2020; 11: 102.
4. Chen DW, Lang BHH, McLeod DSA, Newbold K, Haymart MR. Thyroid cancer. Lancet 2023; 401: 1531-1544.
5. Theotoki EI, Pantazopoulou VI, Georgiou S, Kakoulidis P, Filippa V, Stravopodis DJ, et al. Dicing the disease with Dicer: the implications of dicer ribonuclease in human pathologies. Int J Mol Sci 2020; 21: 7223.
6. Szczyrek M, Grenda A, Kuznar-Kaminska B, Krawczyk P, Sawicki M, Batura-Gabryel H, et al. Methylation of DROSHA and DICER as a biomarker for the detection of lung cancer. Cancers (Basel) 2021; 13: 6139.
7. Stratmann J, Wang CJ, Gnosa S, Wallin A, Hinselwood D, Sun XF, et al. Dicer and miRNA in relation to clinicopathological variables in colorectal cancer patients. BMC Cancer 2011; 11: 345.
8. Tseng CF, Chen LT, Wang HD, Liu YH, Shiah SG. Transcriptional suppression of Dicer by HOXB-AS3/EZH2 complex dictates sorafenib resistance and cancer stemness. Cancer Sci 2022; 113: 1601-1612.
9. Jakymiw A, Patel RS, Deming N, Bhattacharyya I, Shah P, Lamont RJ, et al. Overexpression of dicer as a result of reduced let-7 MicroRNA levels contributes to increased cell proliferation of oral cancer cells. Genes Chromosomes Cancer 2010; 49: 549-559.
10. Meng L, Li H, Fu Y, Yu D, Tang J, Hu Y, et al. Somatic DICER1-mutant benign thyroid nodules in adults: a group of follicular nodular disease with continuous growth. J Clin Endocrinol Metab 2025; 110: 1559-1569.
11. Lee YA, Im SW, Jung KC, Chung EJ, Shin CH, Kim JI, et al. Predominant DICER1 pathogenic variants in pediatric follicular thyroid carcinomas. Thyroid 2020; 30: 1120-1131.
12. Ver Berne J, Van den Bruel A, Vermeire S, De Paepe P. DICER1 mutations define the landscape of poorly differentiated thyroid carcinoma in children and young adults: case report and literature review. Am J Surg Pathol 2024; 48: 1277-1283.
13. Whaley RD, Gupta S, Manninen MC, O'Brien DR, Erickson LA. Clinicopathologic and molecular analysis of 15 pediatric and young adult patients with high-grade non-anaplastic thyroid carcinoma. Endocr Pathol 2024; 35: 397-410.
14. Schiavo Lena M, Sanchez-Ares M, Brunetto E, Abdulkader-Nallib I, Maggiore R, Barbieri D, et al. Focal high-grade areas with a tumor-in-tumor pattern: another feature of pediatric DICER1-associated thyroid carcinoma? Endocr Pathol 2025; 36: 20.
15. Cameselle-Teijeiro JM, Mete O, Asa SL, LiVolsi V. Inherited follicular epithelial-derived thyroid carcinomas: from molecular biology to histological correlates. Endocr Pathol 2021; 32: 77-101.
16. Ramirez-Moya J, Wert-Lamas L, Riesco-Eizaguirre G, Santisteban P. Impaired microRNA processing by DICER1 downregulation endows thyroid cancer with increased aggressiveness. Oncogene 2019; 38: 5486-5499.
17. Penha RCC, Sepe R, De Martino M, Esposito F, Pellecchia S, Raia M, et al. Role of Dicer1 in thyroid cell proliferation and differentiation. Cell Cycle 2017; 16: 2282-2289.
18. Edge SB, Compton CC. The American Joint Committee on Cancer: the 7th edition of the AJCC cancer staging manual and the future of TNM. Ann Surg Oncol 2010; 17: 1471-1474.
19. Cheng CW, Fang WF, Tang KT, Lin JD. The pathogenic role of IFN-alpha in thyroiditis mouse models. Life Sci 2022; 288: 120172.
20. Shamir R, Maron-Katz A, Tanay A, Linhart C, Steinfeld I, Sharan R, et al. EXPANDER – an integrative program suite for microarray data analysis. BMC Bioinformatics 2005; 6: 232.
21. Ke TW, Hsu HL, Wu YH, Chen WT, Cheng YW, Cheng CW. MicroRNA-224 suppresses colorectal cancer cell migration by targeting Cdc42. Dis Markers 2014; 2014: 617150.
22. Cecchini MJ, Amiri M, Dick FA. Analysis of cell cycle position in mammalian cells. J Vis Exp 2012; 21: 3491.
23. Shi JA, Lu DL, Huang X, Tan W. miR-219 inhibits the proliferation, migration and invasion of medulloblastoma cells by targeting CD164. Int J Mol Med 2014; 34: 237-243.
24. Liao Z, Yeo HL, Wong SW, Zhao Y. Cellular senescence: mechanisms and therapeutic potential. Biomedicines 2021; 9: 1769.
25. Hsu TW, Chen HA, Liao PH, Su YH, Chiu CF, Huang CY, et al. Dicer-mediated miR-200b expression contributes to cell migratory/invasive abilities and cancer stem cells properties of breast cancer cells. Aging (Albany NY) 2022; 14: 6520-6536.
26. Kommoss FKF, Chong AS, Chong AL, Pfaff E, Jones DTW, Hiemcke-Jiwa LS, et al. Genomic characterization of DICER1-associated neoplasms uncovers molecular classes. Nat Commun 2023; 14: 1677.
27. Reyes-Castro RA, Chen SY, Seemann J, Kundu ST, Gibbons DL, Arur S. Phosphorylated nuclear DICER1 promotes open chromatin state and lineage plasticity of AT2 tumor cells in lung adenocarcinomas. Sci Adv 2023; 9: eadf6210.
28. Wojcik K, Krzeminska P, Kurzynska-Kokorniak A. Possible role of human ribonuclease dicer in the regulation of R loops. FEBS Open Bio 2025; 15: 1406-1418.
29. Erler P, Keutgen XM, Crowley MJ, Zetoune T, Kundel A, Kleiman D, et al. Dicer expression and microRNA dysregulation associate with aggressive features in thyroid cancer. Surgery 2014; 156: 1342-1350.
30. Paulsson JO, Wang N, Gao J, Stenman A, Zedenius J, Mu N, et al. GABPA-dependent down-regulation of DICER1 in follicular thyroid tumours. Endocr Relat Cancer 2020; 27: 295-308
31. Frezzetti D, Reale C, Cali G, Nitsch L, Fagman H, Nilsson O, et al. The microRNA-processing enzyme Dicer is essential for thyroid function. PLoS One 2011; 6: e27648.
32. Swahari V, Nakamura A, Deshmukh M. The paradox of dicer in cancer. Mol Cell Oncol 2016; 3: e1155006.
33. Luan N, Mu Y, Mu J, Chen Y, Ye X, Zhou Q, et al. Dicer1 promotes colon cancer cell invasion and migration through modulation of tRF-20-MEJB5Y13 expression under hypoxia. Front Genet 2021; 12: 638244.
34. Lai HH, Li JN, Wang MY, Huang HY, Croce CM, Sun HL, et al. HIF-1alpha promotes autophagic proteolysis of Dicer and enhances tumor metastasis. J Clin Invest 2018; 128: 625-643.
35. Ibrahim AA, Schmithals C, Kowarz E, Koberle V, Kakoschky B, Pleli T, et al. Hypoxia causes downregulation of dicer in hepatocellular carcinoma, which is required for upregulation of hypoxia-inducible factor 1alpha and epithelial-mesenchymal transition.Clin Cancer Res 2017; 23: 3896-3905.
36. Xing M. Molecular pathogenesis and mechanisms of thyroid cancer. Nat Rev Cancer 2013; 13: 184-199.
37. Derakhshani A, Rostami Z, Safarpour H, Shadbad MA, Nourbakhsh NS, Argentiero A, et al. From oncogenic signaling pathways to single-cell sequencing of immune cells: changing the landscape of cancer immunotherapy. Molecules 2021; 26: 2278.
38. Ohtani N, Hara E. Roles and mechanisms of cellular senescence in regulation of tissue homeostasis. Cancer Sci 2013; 104: 525-530.

Address for correspondence

Jiunn-Diann Lin, MD
Division of Endocrinology and Metabolism
Department of Internal Medicine
Shuang-Ho Hospital
Taipei, Taiwan
e-mail: jdlin1971@yahoo.com.tw